Bioorganic & Medicinal Chemistry Letters 19 (2009) 4312–4315

Contents lists available at ScienceDirect

Bioorganic & Medicinal Chemistry Letters

journal homepage: www.elsevier.com/locate/bmcl

Structure–activity relationships of memoquin: Influence of the chain chirality in the multi-target mechanism of action

Maria Laura Bolognesi *, Manuela Bartolini, Michela Rosini, Vincenza Andrisano, Carlo Melchiorre

Department of Pharmaceutical Sciences, Alma Mater Studiorum-Bologna University, Via Belmeloro 6, I-40126 Bologna, Italy

ARTICLE INFO

Article history:
Received 22 April 2009
Revised 19 May 2009
Accepted 20 May 2009
Available online 28 May 2009

Keywords:
Alzheimer's disease
Acetylcholinesterase
Butyrylcholinesterase
Amyloid-beta
Small molecule protein-protein interaction inhibitors

ABSTRACT

The present article expands on the study of structure–activity relationships of the novel class of quinone-bearing polyamines, as multi-target-directed ligands against Alzheimer's disease. Namely, the effect of inserting a methyl substituent at the α position of the terminal benzyl amine moieties of lead candidate **1** (memoquin) was evaluated at the multiple targets involved in the multifunctional mechanism of action. The *RR* stereoisomer **2** resulted more effective than **1** in reverting two important effects mediated by acetylcholinesterase (AChE), that is, acetylcholine hydrolysis and AChE-induced amyloid-β aggregation.

Despite the huge research effort and the considerable strides already made, Alzheimer's disease (AD) still is an incurable pathology which provokes considerable concern inside the pharmaceutical community.[1,2] Over the past decade, trying to address the pitfalls that have long hindered the identification of effective therapeutic tools, we developed an innovative concept, which embodies in the design of Multi-Target Directed Ligands (MTDLs) as response to the multifactorial nature of AD.[3] This approach has proven particularly fruitful and allowed the identification of several MTDLs, some of which have emerged as interesting pharmacological tools for the investigation of neurodegenerative disorders, or as innovative drug candidates for combating AD.[3–5]

Among them, memoquin (**1**) is a promising new chemical entity that has been rationally designed with the deliberate aim of creating a multifunctional small molecule acting at different levels of the neurodegenerative cascade underlying AD pathology.[6]

By inserting the antioxidant benzoquinone moiety of the promising drug candidate ubiquinone (2,3-dimethoxy-5-methyl-6-decaprenyl-1,4-benzoquinone) into a polyamine scaffold endowed with acetylcholinesterase (AChE) inhibition activity **1** was generated (Fig. 1). An in-depth in vitro and in vivo characterization has confirmed its multifunctional mechanism of action and verified the interaction of **1** with different crucial molecular targets in AD neurotoxic pathways, such as AChE and β-secretase (BACE-1) enzymes, β-amyloid (Aβ) and oxidative processes.[7] The ability of **1** to exert a positive pharmacological effect on AD neurodegeneration in vivo was verified by extending the studies to different animal models for AD.[7] Administration of **1** to anti NGF AD11 mice showed that it is able to ameliorate neuropathological signs and cognitive deficits, confirming its capability to impinge on different points of the cascade/s leading to neurodegeneration.[6,7]

In a search of memoquin derivatives with an improved MTDL profile, we previously synthesized a small unbiased library of **1**-derivatives, and analyzed the contributions of the different

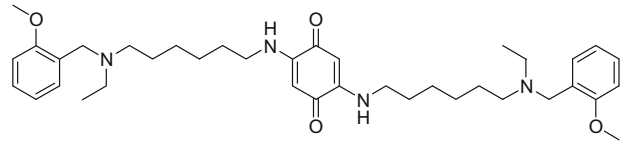

1

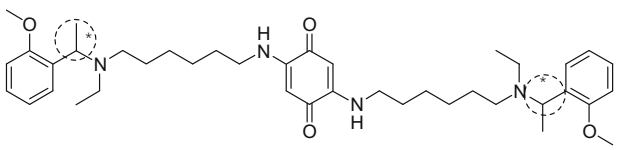

2: *RR*
3: *SS*
4: *RS*

Figure 1. Chemical structures of **1** and its chiral derivatives **2–4**.

* Corresponding author. Tel.: +39 051 2099718; fax: +39 051 2099734.
E-mail address: marialaura.bolognesi@unibo.it (M.L. Bolognesi).

0960-894X/$ - see front matter © 2009 Elsevier Ltd. All rights reserved.
doi:10.1016/j.bmcl.2009.05.087

structural elements to the different activities.[8] The data obtained from this SAR study confirmed that **1** was indeed the best ligand targeting the different biological targets relevant in the AD pathology. However, the resulting information, in addition to the molecular modeling studies on **1**, allowed us to hypothesize some further structural manipulation potentially leading to lead optimization. Therefore, starting from the **1**-AChE complex obtained by docking simulations,[7] and being aware that AChE peripheral and catalytic sites are rich in hydrophobic aminoacids, we explored the introduction of a methyl substituent at the α position of the terminal benzyl amine moieties. Due to the symmetrical nature of **1**, this modification generates two equivalent stereogenic centers, and three possible stereoisomers: the pair of enantiomers **2** and **3** and the *meso* stereoisomer **4**, as shown in Figure 1.

Chiral discrimination has tremendous importance in medicinal chemistry as a means to gain insight into the mechanisms of interaction and to better understand structural features of ligand-target recognitions.

On the basis of this rational design, **2–4** should possess a better inhibition profile against AChE and more importantly, could bind more tightly to the allosteric peripheral anionic site (PAS) of AChE, with a concomitant higher prevention of AChE-promoted Aβ aggregation. The theory that AChE acts as a pathologic chaperone, accelerating the formation of amyloid fibrils in the brain and forming stable complexes with Aβ at the PAS region, has found general acceptance.[9,10]

Consequently, AChE has been recently revaluated as a key target for AD drug discovery.[11–14]

The *RR*, *SS* and *RS-meso* isomers **2–4** have been separately synthesized, by exploiting a route different from the standard synthetic protocol used for memoquin.[8] Commercial availability of both (1*R*)- and (1*S*)-1-(2-methoxyphenyl)ethanamines (**5** and **6**) prompted us to use them as chiral building blocks. They were *N*-ethylated by a reductive amination procedure (**7** and **8**) and then alkylated by reaction with (6-chloro-hexyl)-carbamic acid *tert*-butyl ester.[15] The obtained intermediates **9** and **10** were deprotected at the terminal amino function to get the required diamines **11** and **12** (Scheme 1). Afterward, in the case of **2** and **3** the reaction scheme proceeds as reported for **1**,[8] exploiting the efficient substitution reaction on 2,5-dimethoxybenzoquinone (**13**). Conversely, for the synthesis of the *meso* derivative **4**, we optimized monosubstitution reaction conditions on **13** by reacting an excess of it with diamine **11**, and isolating the monosubstituted derivative **14** in acceptable yield. Then, the remaining methoxy group of **14** was displaced by the primary amino group of **12**, affording the final *meso* compound **4** (Scheme 2).[16]

The influence of chirality of memoquin and other MTDLs at the different molecular targets has never been explored before. Therefore, this investigation was directed toward evaluating changes in the polypharmacological profile resulting from introducing chirality into the terminal benzyl groups of **1**. We thought to preliminary disclose the effect of this modification on chiral protein targets such as AChE, BChE and Aβ. We assumed that this effect would be negligible on the antioxidant profile, as trolox equivalent antioxidant capacity (TEAC) is mediated by the quinone moiety.[7,8]

To determine the biological profile of **2–4** as MTDLs for the treatment of AD, they were screened at the four selected targets, that is, (a) AChE and BChE, (b) Aβ aggregation induced by human recombinant AChE, (c) self-induced Aβ aggregation, using experimental procedures reported before.[8,10,17] To allow comparison of the results, **1** was used as reference compound. From the data reported in Table 1 some interesting conclusions can be drawn; AChE inhibition can be affected by the introduction of a methyl group on the benzyl moiety of **1** and chirality of this stereocenter modulates AChE activity. Specifically, the inhibitory potency of the *RR* enantiomer **2** and the *meso* **4** resulted slightly improved with respect to that of **1**, reaching values in the sub-nanomolar range. Notably, being endowed with an IC_{50} value of 0.36 nM, **4** emerges as the most active AChE inhibitor among **1**-derivatives developed so far. Conversely, the *SS* enantiomer **3** was 2.6-fold less potent than **1**.

Regarding the inhibitory profile against human BChE, all the stereoisomers maintained, although at a different extent, the remarkable selectivity displayed by the prototype **1**. Despite no significant differences in the IC_{50} values against BChE for the different enantiomers might be found, the overall BChE/AChE selectivity ratio for **2** and **3** differs of one order of magnitude (2960 vs 238). This is due to the different trend in activities for **2** and **3** towards the two target proteins.

In parallel to the improved activity profile against human AChE, the new derivatives showed a better efficacy in inhibiting the AChE pro-aggregating action. As shown in Table 2, compounds **2–4** blocked the amyloid aggregation induced by AChE with IC_{50} values

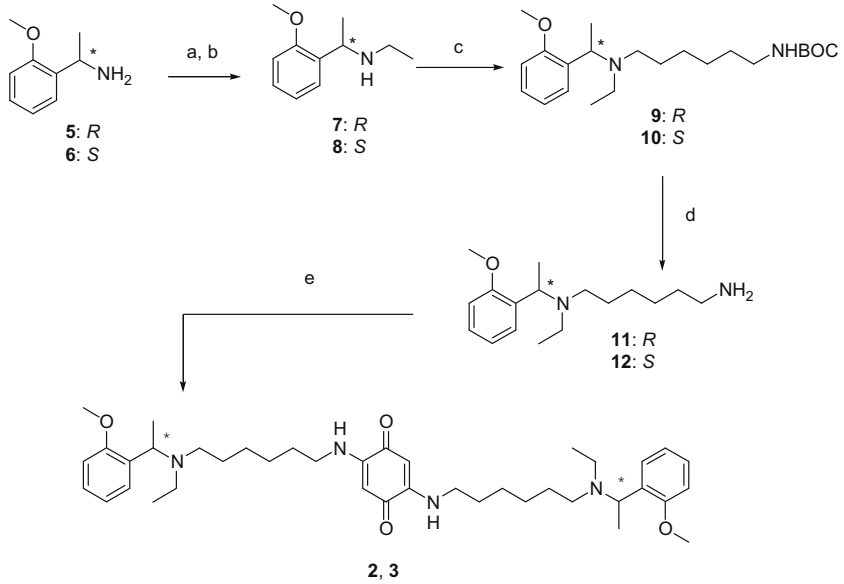

Scheme 1. Reagents and conditions: (a) 1.1 equiv CH_3CHO, EtOH, 3 h, rt; (b) $NaBH_4$, 12 h, rt; (c) 2 equiv (6-chlorohexyl)carbamic acid *tert*-butyl ester, 8 equiv KI, 4 equiv $EtN(iPr)_2$, EtOH, reflux, 48 h; (d) TFA, 2H, rt; (e) 0.5 equiv **13**, EtOH, 50 °C for 3 h, then rt, overnight.

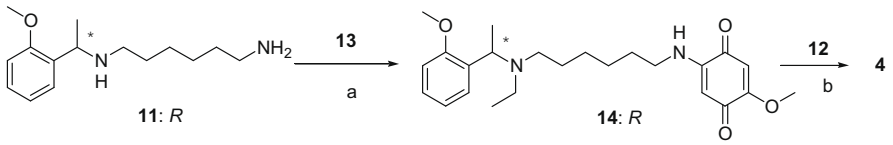

Scheme 2. Reagents and conditions: (a) 7 equiv **13**, $CHCl_3$/EtOH, 50 °C for 10′, then rt overnight; (b) 1 equiv **13**, CH_2Cl_2, rt, overnight.

Table 1
Inhibition of AChE and BChE activities, by **2**–**4** and reference compound **1**

Compd		IC_{50} (nM)[a]		
		AChE	BChE	BChE/AChE[b]
1[c]	—	1.55 (±0.11)	1440 (±100)	929
2	*R,R*	0.50 (±0.02)	1480 (±40)	2960
3	*S,S*	4.03 (±0.20)	958 (±18)	238
4	*R,S*	0.36 (±0.02)	982 (±37)	2728

[a] Values are mean of three experiments, standard deviation is given in parentheses.
[b] The AChE/BChE selectivity ratio is the ratio of IC_{50} values at BChE and AChE, respectively.
[c] From Ref. 7.

lower than that displayed by the drug candidate **1**. Remarkably, **3** was the most potent in the series and resulted 3.6-fold more efficient than **1**. Nevertheless, **2** resulted only slightly less potent than **3**. The most potent published compounds acting as AChE-induced Aβ aggregation inhibitors display a potency in the same range as **3** and **2**.[18–21] As verified in other cases, these profiles do not perfectly parallel the relative AChE inhibitory activities. In fact, **3** displayed a higher anti-aggregating activity with respect to **1**, **2** and **4**, despite its lower AChE inhibitory potency. Figure 2 shows the inhibition profile obtained for compound **2** in the thioflavin T florescence-based assay for the anti-aggregating potency determination.

Concerning amyloid self-induced aggregation, compounds were screened at the same concentration used for characterizing **1** (10 μM). The almost identical inhibition percentage provided by **2–4** with respect to **1** points to the conclusion that the presence of additional substituents on the benzyl moiety is irrelevant against the self-induced Aβ aggregation. Notably, also **2–4** emerge as small molecule capable to inhibit protein–protein interaction in AD. It is also highly conceivable that they share with **1** the same anti-amyloidogenic mechanism of action, by binding to Aβ in the prevailing β-sheet conformation and by preventing the induction of the conformational shift on vicinal peptides.[17]

In conclusion, owing to the improved inhibitory potency against AChE and AChE-induced aggregation, **2** is the first memoquin derivative showing a better MTDL profile; in particular **2** is more effective than **1** in altering two important effects in AD neurotoxic cascade mediated by AChE (prevention of Aβ fibrils formation in addition to simple inhibition of acetylcholine hydrolysis). From these results, **2** emerges as a small-molecule-based MTDL that can serve as powerful tool both in understanding the role and function of the multiple biological targets and in further validating the design rationale.

Table 2
Inhibition of AChE-mediated and self-induced Aβ aggregation by **2**–**4** and reference compound **1**

Compd		Inhibition of Aβ aggregation[a]	
		AChE-induced IC_{50}[b] (μM)	Self-induced[c] (%)
1[d]	—	28.3 (±0.3)	66.8 (±4.4)
2	*R,R*	9.34 (±1.42)	63.9 (±1.4)
3	*S,S*	7.91 (±0.69)	62.3 (±0.3)
4	*R,S*	11.0 (±1.4)	63.5 (±2.0)

[a] Values are mean of three experiments, standard deviation is given in parentheses.
[b] Inhibition of AChE-induced Aβ(1–40). The Aβ(1–40)/AChE ratio was equal to 100:1.
[c] Inhibition of self-induced Aβ(1–42) aggregation (50 μM) produced by the tested compound at 10 μM concentration.
[d] From Ref. 7.

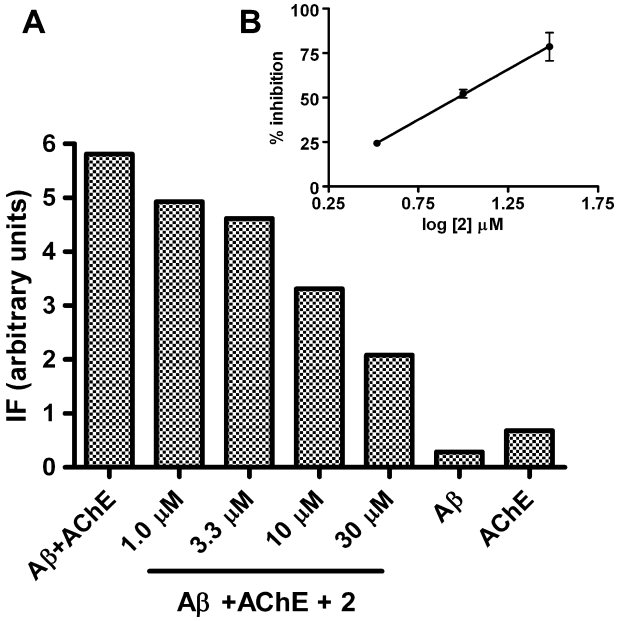

Figure 2. Inhibition of AChE-induced Aβ aggregation by **2**. (A) Bar plot showing experimental florescence values obtained for AChE-induced Aβ aggregation in the absence and in the presence of increasing concentrations of inhibitor. AChE and Aβ florescence values are used as blanks. (B) Inhibition plot. When measuring the AChE-mediated aggregation, the concentration of Aβ(1–40) was 230 μM, whereas the Aβ(1–40)/AChE ratio was equal to 100:1.

Acknowledgement

This work was supported by the University of Bologna. Federica Lizzi, Fabio Magnani and Ioannis Matziris are acknowledged for excellent technical assistance.

References and notes

1. Abbott, A. *Nature* **2008**, *456*, 161.
2. Gura, T. *Nat. Med.* **2008**, *14*, 894.
3. Cavalli, A.; Bolognesi, M. L.; Minarini, A.; Rosini, M.; Tumiatti, V.; Recanatini, M.; Melchiorre, C. *J. Med. Chem.* **2008**, *51*, 347.
4. Bolognesi, M. L.; Minarini, A.; Rosini, M.; Tumiatti, V.; Melchiorre, C. *Mini-Rev. Med. Chem.* **2008**, *8*, 960.
5. Bolognesi, M. L.; Rosini, M.; Andrisano, V.; Bartolini, M.; Minarini, A.; Tumiatti, V.; Melchiorre, C. *Curr. Pharm. Des.* **2009**, *15*, 601.
6. Bolognesi, M. L.; Cavalli, A.; Melchiorre, C. *Neurotherapeutics* **2009**, *6*, 152.
7. Cavalli, A.; Bolognesi, M. L.; Capsoni, S.; Andrisano, V.; Bartolini, M.; Margotti, E.; Cattaneo, A.; Recanatini, M.; Melchiorre, C. *Angew. Chem., Int. Ed.* **2007**, *46*, 3689.
8. Bolognesi, M. L.; Banzi, R.; Bartolini, M.; Cavalli, A.; Tarozzi, A.; Andrisano, V.; Minarini, A.; Rosini, M.; Tumiatti, V.; Bergamini, C.; Fato, R.; Lenaz, G.; Hrelia, P.; Cattaneo, A.; Recanatini, M.; Melchiorre, C. *J. Med. Chem.* **2007**, *50*, 4882.

9. Inestrosa, N. C.; Alvarez, A.; Perez, C. A.; Moreno, R. D.; Vicente, M.; Linker, C.; Casanueva, O. I.; Soto, C.; Garrido, J. *Neuron* **1996**, *16*, 881.
10. Bartolini, M.; Bertucci, C.; Cavrini, V.; Andrisano, V. *Biochem. Pharmacol.* **2003**, *65*, 407.
11. Castro, A.; Martinez, A. *Curr. Pharm. Des.* **2006**, *12*, 4377.
12. Holzgrabe, U.; Kapkova, P.; Alptuzun, V.; Scheiber, J.; Kugelmann, E. *Expert Opin. Ther. Targets* **2007**, *11*, 161.
13. Munoz-Torrero, D. *Curr. Med. Chem.* **2008**, *15*, 2433.
14. Inestrosa, N. C.; Dinamarca, M. C.; Alvarez, A. *FEBS J.* **2008**, *275*, 625.
15. Bolognesi, M. L.; Bixel, M. G.; Marucci, G.; Bartolini, M.; Krauss, M.; Angeli, P.; Antonello, A.; Rosini, M.; Tumiatti, V.; Hucho, F.; Melchiorre, C. *J. Med. Chem.* **2002**, *45*, 3286.
16. *Spectral data for target compounds*. Compounds **2** and **3**: red solids, mp 63–65 °C; ^{1}H NMR (300 MHz,$CDCl_3$) d 1.02 (6H, t, *J* = 7.0 Hz, CH_2CH_3), 1.29 (6H, d, *J* = 6.9 Hz, $CHCH_3$), 1.27–1.64 (16H, m complex, aliphatic chain), 2.38–2.76 (8H, m complex, CH_2N) 3.13 (4H, q, *J* = 6.4 Hz, $NHCH_2$), 3.83 (6H, s, OCH_3), 4.32 (2H, q, *J* = 6.9 Hz, $CHCH_3$), 5.31 (2H, s, quinone), 6.61 (2H, br t exch with D_2O, NH), 6.88 (2H, d, *J* = 8 Hz, ArH), 6.95 (2H, t, ArH), 7.20 (2H, t, *J* = 9 Hz, ArH), 7.45 (2H, d, *J* = 9 Hz, ArH); ESI-MS (*m/z*): 662 ($M+H^+$). Compound **4**: red waxy solid; ^{1}H NMR (300 MHz,$CDCl_3$) d 1.01 (6H, t, *J* = 7.0 Hz, CH_2CH_3), 1.17–1.84 (22H, m complex, aliphatic chain + $CHCH_3$), 2.33–2.96 (8H, m complex, CH_2N), 3.13 (4H, q, *J* = 6.4 Hz, $NHCH_2$), 3.86 (6H, s, OCH_3), 4.42–4.75 (2H, m, $CHCH_3$), 5.30 (2H, s, quinone), 6.59 (2H, br t exch with D_2O, NH), 6.90 (2H, d, *J* = 8 Hz, ArH), 6.95 (2H, t, *J* = 7.8 Hz, ArH), 7.20 (2H, t, *J* = 8 Hz, ArH), 7.45 (2H, d, *J* = 8 Hz, ArH); ESI-MS (*m/z*): 662 ($M+H^+$). Chiral purity has been verified converting diamine **2–4** into the corresponding diasteromeric salts with *S*-Mosher acid (*S*-α-methoxy-α-(trifluoro-methyl)phenylacetic acid), and analyzing their enantiomeric composition by 400 MHz ^{1}H NMR spectroscopy.
17. Bartolini, M.; Bertucci, C.; Bolognesi, M. L.; Cavalli, A.; Melchiorre, C.; Andrisano, V. *ChemBioChem* **2007**, *8*, 2152.
18. Bolognesi, M. L.; Andrisano, V.; Bartolini, M.; Banzi, R.; Melchiorre, C. *J. Med. Chem.* **2005**, *48*, 24.
19. Munoz-Ruiz, P.; Rubio, L.; Garcia-Palomero, E.; Dorronsoro, I.; del Monte-Millan, M.; Valenzuela, R.; Usan, P.; de Austria, C.; Bartolini, M.; Andrisano, V.; Bidon-Chanal, A.; Orozco, M.; Luque, F. J.; Medina, M.; Martinez, A. *J. Med. Chem.* **2005**, *48*, 7223.
20. Tumiatti, V.; Milelli, A.; Minarini, A.; Rosini, M.; Bolognesi, M. L.; Micco, M.; Andrisano, V.; Bartolini, M.; Mancini, F.; Recanatini, M.; Cavalli, A.; Melchiorre, C. *J. Med. Chem.* **2008**, *51*, 7308.
21. Xie, Q.; Wang, H.; Xia, Z.; Lu, M.; Zhang, W.; Wang, X.; Fu, W.; Tang, Y.; Sheng, W.; Li, W.; Zhou, W.; Zhu, X.; Qiu, Z.; Chen, H. *J. Med. Chem.* **2008**, *51*, 2027.